Published in final edited form as:
J Morphol. 1999 November ; 242(2): 167. doi:10.1002/(SICI)1097-4687(199911)242:2<167::AID-JMOR8>3.0.CO;2-1.

Craniofacial Sutures: Morphology, Growth, and In Vivo Masticatory Strains

KATHERINE L. RAFFERTY* and **SUSAN W. HERRING**
University of Washington, Department of Orthodontics, Seattle, Washington

Abstract

The growth and morphology of craniofacial sutures are thought to reflect their functional environment. However, little is known about in vivo sutural mechanics. The present study investigates the strains experienced by the internasal, nasofrontal, and anterior interfrontal sutures during masticatory activity in 4–6-month-old miniature swine (*Sus scrofa*). Measurements of the bony/fibrous arrangements and growth rates of these sutures were then examined in the context of their mechanical environment. Large tensile strains were measured in the interfrontal suture (1,036 με ± 400 SD), whereas the posterior internasal suture was under moderate compression (−440 με ± 238) and the nasofrontal suture experienced large compression (−1,583 με ± 506). Sutural interdigitation was associated with compressive strain. The collagen fibers of the internasal and interfrontal sutures were clearly arranged to resist compression and tension, respectively, whereas those of the nasofrontal suture could not be readily characterized as either compression or tension resisting. The average linear rate of growth over a 1-week period at the nasofrontal suture (133.8 μm, ± 50.9 S.D) was significantly greater than that of both the internasal and interfrontal sutures (39.2 μm ± 11.4 and 65.5 μm ± 14.0, respectively). Histological observations suggest that the nasofrontal suture contains chondroid tissue, which may explain the unexpected combination of high compressive loading and rapid growth in this suture.

Keywords

sutures; mastication; bone strain; skull; growth; miniature swine

Previous work has shown that some cranial sutures experience large strains during normal mastication (Herring and Mucci, ’91; Herring and Teng, submitted). Strains of 1,000–2,000 microstrain in the zygomatic sutures (Herring and Mucci, ’91) are comparable in magnitude to those measured in the postcranial skeleton during vigorous locomotion (Biewener and Taylor, ’86) and are much larger than those measured in adjacent cranial bones. Mechanical tests on goat crania have revealed that areas of bone with sutures absorb more energy under impact loading than cranial bone alone, and that the amount of energy absorption increases with sutural interdigitation (Jaslow, ’90). The limited data we have on functional cranial suture strains suggest that adjacent sutures may experience large magnitude strains of opposite polarity (tension and compression) and that the predominant loading patterns may be associated with specific suture morphologies. For example, the vertical portion of the pig zygomatic suture is in compression and the horizontal portion is in tension during mastication and masseter stimulation. Well-developed interdigitating contacts of zygomatic and squamosal bone with compression-resisting fibers are found in the vertical segment, whereas the horizontal portion of these two contacting bones has a much simpler interface with tension-resisting fibers

*Correspondence to: Katherine L. Rafferty, Ph.D., University of Washington, Department of Orthodontics, Box 357446, Seattle, WA 98195-7446. kraff@u.washington.edu.

(Herring and Mucci, ’91). Interdigitating projections of bone serve to increase the surface area for collagen fiber attachment as well as provide areas for obliquely arranged, compression-resisting fibers to attach (Herring, ’72; Jaslow, ’90).

An important question is how, or if, the patterns of growth at sutural margins are interrelated with their bony/fibrous morphologies and ultimately, their functional environments. Although cranial sutures do form in the absence of muscle activity (Persson, ’83), numerous studies support Moss’ hypothesis (’57) that the fine details of suture morphology, such as interdigitation, are secondary responses to extrinsic forces. Transposition of portions of the coronal and sagittal suture and inversion of a suture result in an adoption of the characteristic morphology of the new location (Markens and Oudhof, ’80; Oudhof, ’82). Also, masticatory muscle resection and surgical isolation and mechanical immobilization of portions of sutures result in loss of sutural complexity (Moss, ’61; Koskinen, ’77; Foley and Kokich, ’80). As yet, very little is known about how the forces generated during chewing influence the growth at suture margins and the subsequent development of sutural complexity and fiber organization. An extensive literature exists on the tissue responses to the application of abnormal extrinsic forces (see summaries by Wagemans et al., ’88; Kokich, ’92). In short, the application of increased compression and tension via the use of orthodontic devices leads to resorption/reduced deposition and increased apposition, respectively, at sutural margins. However, it is not known if sutural tissue responds similarly to the polarity of normal functional strains during growth.

The present study was undertaken to investigate the interrelationships among growth, morphology, and in vivo strains of the sutures of the pig rostrum and anterior braincase (internasal, nasofrontal, and anterior interfrontal sutures). The rostral area was chosen because of its rapid growth in later development (Todd and Cooke, ’34) and because strains in this area have never been investigated in any species. Based on our previous work on the zygomatic suture (Herring and Mucci, ’91), we predict that sutures that predominantly experience compressive loading will exhibit a greater degree of interdigitation than sutures under a predominantly tensile load, and that collagen fibers will be arranged to resist these forms of stress. A schematic drawing of a compressed and tensed suture with the theoretical interdigitation and suture fiber arrangements is provided in Figure 1. Further, based on previous work with extrinsic loads (Wagemans et al., ’88; Kokich, ’92), we expect that sutural growth rates will be lower in those sutures experiencing predominant compression than in those under predominant tension during normal function (mastication). These predictions are somewhat at odds with the notion that complex interdigitations are a means of expediting rapid growth (Koskinen et al., ’76), a contradiction also noted by Oudhof (’82), who posed the question as to whether the lingulae of interdigitating sutures are of immediate significance for growth or a secondary product of mechanical stresses.

MATERIALS AND METHODS

Six Hanford strain miniature pigs (*Sus scrofa*), obtained from Charles River Laboratories (Wilmington, MA), were used in this study. All experimental procedures were approved by the University of Washington Animal Care Committee. The experimental animals ranged in age from 4–6 months and weighed 13–27 kg (Table 1). Double fluoro-chrome labels were given to the subjects prior to surgery and data collection to act as time markers in measurements of sutural growth. Calcein (Sigma, St. Louis, MO) was given via intravenous injection 7 days prior to the experiment (12.5 mg/kg calcein in a 5 mg/ml solution of pyrogen-free water neutralized with a 1 N solution of NaOH and filtered with a .22 μm syringe filter). A similar procedure was carried out with the second label, demeclocycline (Sigma), which was given 5 days later in a neutralized and filtered solution (15 mg/kg demeclocycline in 10 mg/ml ddH_20).

On the day of the experiment the subjects were anesthetized with halothane and nitrous oxide. The skin of the rostrum was incised close to midline and retracted. The periosteum was reflected, exposing a window of bone and sutures, which was prepared by a succession of cautery, scraping, degreasing, conditioning, buffering, and drying. Once the surfaces were prepared, a narrow (1–2 mm) strip of Teflon was placed immediately over each cranial suture (to prevent gluing the suture margins together) and single element strain gauges (EP-08–125BT-120; Measurements Group, Raleigh, NC) capable of measuring uniaxial strain (compression/tension) were glued perpendicular to the sutures of interest using cyanoacrylate (see Fig. 2 and Table 1 for gauge locations). Although uniaxial gauges cannot give information about the magnitude and direction of principal strains, it proved to be impossible to use three-element rosette gauges in these locations because the stiffer rosettes buckled rather than followed the distortions of the suture. The uniaxial gauges accurately report the polarity of strains (tension or compression), but shearing components exaggerate tensile magnitude and reduce compressive magnitude. After verifying that the gauges were operational by achieving a balance using Measurements Group Model 2120A strain gauge conditioners and amplifiers, the periosteum and skin were separately sutured. The lead wires with an attached plug were exited from the wound and were secured to a collar around the neck. A topical anesthetic (2% procaine hydrochloride) was drizzled on the incision and an analgesic (buprenorphine hydrochloride) was given by injection prior to the recording session.

After surgery, but with the animals still under anesthesia, fine-wire electromyography electrodes were placed in the bilateral masseter and temporalis muscles (method described in Herring and Mucci, ’91). The subjects were allowed to wake up from anesthesia and were offered water and their normal diet of pig chow. EMG signals were led to high-impedance probes (model 7HIP5G; Grass Instrument, Quincy, MA) and then amplified (Grass, 7P3C). The amplified strain and EMG signals were then converted to digital signals (MP100, Biopac Systems, Santa Barbara, CA) and input into a Power Macintosh running Acqknowledge III (Biopac Systems). Strain and EMG data were collected at a rate of 500 Hz for 10–20 min of mastication. Subjects were then reanesthetized. Thirty minutes prior to being euthanized, they were injected with 3,000 units of heparin i.p. Euthanasia by intracardiac injection of pentobarbital was followed immediately by carotid perfusion with 2 to 3 liters of heparinized saline followed by about 4 liters of 10% neutral buffered formalin.

Analysis of strain data was accomplished by transferring waveform data from Acqknowledge into Microsoft Excel, where they were zeroed and converted to microstrain. Peak strains were extracted for each masticatory cycle for several series of chews. The EMG pattern was used primarily to determine the side of chewing (see Huang et al., ’93). However, in most pigs the side of chewing had no effect on peak strain. In two animals (254 and 255), differences in strain were seen in an alternating pattern, suggesting that chewing side was responsible. However, EMG was not of sufficient quality to identify the side of chewing in these two animals, so an equal number of each of the two patterns were measured and averaged.

Cores of bony tissue at the suture gauge locations were removed from the formalin-fixed skulls, stripped completely of soft tissue, and placed in 70% ETOH for storage. Specimens were allowed to dry, attached to plastic stubs with epoxy, and sectioned at a thickness of 60–70 μm with a Leica SP1600 saw microtome. As several sections were made from each sample, some were mounted on slides with Permount (Fischer Scientific; Fair Lawn, NJ) and coverslipped while others were allowed to dry flat on the slide. Sections were not stained. In addition to these procedures, a small sample of specimens was decalcified, embedded in paraffin, sectioned to 7–10 μm, and stained with hematoxylin and eosin.

Mineralized sections were viewed with either a fluorescent/light microscope (Nikon Eclipse E400) or a dissection scope (Nikon SMZ-U), and digital images were obtained using an

attached video camera and NIH Image software. Linear calibrations were included in all of the images. A rough measure of suture complexity was obtained by measuring the true length of the suture by tracing its entire course from the endo- to ectocranial surfaces and dividing this length by the shortest distance between the suture's openings onto the endo- and ectocranial surfaces. This measure is analogous to that used by Jaslow ('89) and Anton et al. ('92) to measure ectocranial suture complexity. Using this ratio, more complex, deeply interdigitated sutures will have larger values than less complex sutures. In the thick, undecalcified sections, sutural fibers were best observed using the fluorescent mode (wavelength 450–490 nm). Sutural fibers were also observed in the stained thin sections using light microscopy.

Because repeated exposure to UV light degrades the fluorescent image intensity, different mineralized sections were used in the study of sutural growth. Sutural growth was assessed by measuring the area of labeled bone at the suture margins. A series of overlapping images of parts of a suture were digitally captured and constructed into a montage of the entire suture. The labeled bone in areas other than the suture margins was removed from the image. A count of all pixels in the range of gray scale values characteristic of the labeled bone was obtained and the known relationship of pixel/mm^2 allowed a simple conversion to area of labeled bone. The only problem with this method was that the second label (demeclocycline) was sometimes hard to distinguish. Therefore, this total area may slightly underestimate the labeled area of bone (but not systematically more in any one suture location). In order to make comparisons within and between individuals, the area of labeled bone was standardized by dividing by the entire (true) length of the suture (the sum of the lengths of the two suture margins). This measurement gives a measure of the average linear amount of bone deposited during the two labeling periods.

This method worked well with the internasal and interfrontal sutures but was not appropriate for the nasofrontal suture. The labeled bone of the nasofrontal suture had a much different texture from that in the other sutures, and it was not always possible to delineate the borders of labeled bone adjacent to the suture space. Therefore, several direct linear measurements were made on each specimen of the width of labeled bone perpendicular to the suture margin. Only the regions of the suture margin between the tips of the interdigitating processes, and not the tips themselves, were measured. Because relatively more labeled bone was present at the interdigitating tips, this measure of average linear growth is a minimum estimate. We examined the comparability of these techniques by measuring the labeled bone of the interfrontal and posterior internasal suture using the direct linear method in two individuals (243, 253). We found that in each suture this method gave lower estimates of growth (by 30–47%) compared to the method that utilized the total area of labeled bone. However, linear regression of the measurements derived from the two methods (n = 4) indicated that they are highly correlated ($r^2 = 0.997$).

RESULTS

Suture strains during function

Suture strains recorded during mastication are shown in Figures 3 and 4 and in Table 2. Masticatory function appeared normal and unchanged by strain gauge instrumentation in four out of the six pigs. These four animals woke quickly from anesthesia and ate enthusiastically. The other two, pigs 243 and 253, remained drowsy and were not interested in food. However, both of these animals chewed readily on objects such as tongue depressors and plastic tubing and strain data were collected during these behaviors. Strain data from pigs 243 and 253 were included in the analysis because they were found to be of similar magnitude and polarity when compared to data from the other pigs.

The magnitudes of the sutural strains for a series of chewing cycles were consistent within individual pigs; coefficients of variation were usually 30% or below (data in Table 2). By convention, compression is negative and tension is positive. Among pigs the sutural strains were consistent in terms of polarity (tension vs. compression) and in terms of general patterns of strain magnitude, although absolute magnitudes at specific locations were more variable. In four of the six pigs the chewing side had no effect on the suture strain patterns, even for the bilateral nasofrontal sutures. However, pigs 254 and 255 each showed two distinct strain patterns, presumably related to chewing side. Unfortunately, EMG for these animals was too poor to allow the chewing side to be distinguished.

The strain data indicate that adjacent sutures experience strikingly different strain patterns during normal mastication (Table 2). Figure 3 shows a typical raw strain recording for the sutures of interest and Figure 4 provides an overall summary of analyzed strains. In all of the pigs, and in agreement with our previous work on more posterior locations (Herring and Teng, submitted), the interfrontal suture was in tension during chewing (1,036 με ± 400 S.D.). Not only were the peak strains tensile, but the strains in the interfrontal suture were tensile throughout the chew cycle. In contrast, all sutures involving the nasal bones registered compression. Strains recorded from the posterior internasal gauge site (no more than 2.5–3.0 cm anterior to the interfrontal suture gauge site, Fig. 2) were the least compressive (−440 με ± 238), and the right side chews in pig 254 actually produced very low tensile strain (<100 με). The two pigs with gauge sites in the midinternasal suture (~1–2 cm anterior to the posterior internasal suture) both showed a trend of increasing compressive suture strain from posterior to anterior (Table 2). Very large compressive peak strains were recorded during mastication from the nasofrontal suture of all the pigs (−1,583 με ± 506), although some animals showed small tension in this suture in the early part of the chew cycle.

Suture morphology

A summary of cranial suture complexity, as expressed in the interdigitation index (see Materials and Methods) is provided in Table 3. Photographs of histological sections of sutures under low magnification are provided in Figure 5. Gross anatomical examination of the medial surface of the nasal bones revealed a series of thin, transversely (horizontally) oriented plates of bone that interdigitated at the internasal suture. Histological sections showed this suture as a highly convoluted space weaving around these bony projections (Fig. 5a). The interdigitation index was 1.8–3.4 for the internasal suture (combined mean of 2.44). Although the sample size was too small for statistics, the index was highest at the middle site, intermediate at the posterior site, and lowest at the anterior site of the internasal suture. The interdigitations in the anterior interfrontal suture were also found to be transversely oriented, and in all individuals but one (pig 252) the interdigitations were less pronounced than in the internasal suture, as was reflected in the interdigitation index (Table 3, *P*Fig. 5b). Finally, the nasofrontal suture had a highly complex bony arrangement. The nasal bone overlapped the frontal bone and each bone contributed numerous long interdigitating plates that were oriented roughly parasagittally. It was not always possible to obtain histological sections that were perpendicular to the suture and thus it was not always possible to follow the suture from the dorsal to the ventral surface (but see Fig. 5c). However, the sections with complete nasofrontal sutures had high interdigitation indices (mean of 4.0), significantly greater than those of the internasal and interfrontal sutures (ANOVA/Tukey: = 0.005 and P = .001, respectively). Although the internasal and interfrontal sutures were not significantly different from each other in interdigitation using analysis of variance, the fact that only one individual had an interdigitation index value for the interfrontal suture that fell within the internasal range suggests a trend of increasing interdigitation from the interfrontal to internasal to nasofrontal.

Figure 6 shows a series of close-up pictures that demonstrate the arrangement of collagen fibers within the internasal, interfrontal, and nasofrontal sutures. The following descriptions of collagen fiber orientation within the sutural ligament are based on observations of four interfrontal sutures, four posterior internasal sutures, two anterior internasal sutures, three middle internasal sutures, and four nasofrontal sutures. Not all locations were originally sampled in all of the subjects, and some of those that were did not adequately preserve the suture fiber structure.

In all three locations of the internasal suture (anterior, middle, and posterior) the suture fibers had a similar pattern. Fibers were loosely dispersed and spanned the suture space diagonally (Fig. 6a). Many fibers crossed the space, either directly or by networking in a central vascular zone, and attached to the suture margins. The pattern is the one depicted in Figure 1A, the predicted configuration for resisting compressive force. That is, if the two internasal bones were pushed together, the fibers of the suture are arranged to become taut. There was little evidence of discrete attachments at the corners where the suture wraps around a bony projection.

The fibers within the interfrontal suture had a distinctly different pattern from those of the internasal suture. In thick sections the sutural fibers appeared more centrally consolidated in the suture space and wound around the projections of bone, often attaching to them. At these projections, collagen fibers were observed to radiate from the central region to the opposing surfaces in both thick sections and H&E-stained thin sections. In the areas between interdigitating processes, collagen fibers also extended from the central region into both sides of the suture margin, as seen in Figure 6b. This arrangement resembles that predicted for tension resistance in Figure 1B.

Sagittal sections proved inadequate to assess fiber orientation in the nasofrontal suture. Whereas the interfrontal and internasal sutures showed the same pattern among individuals, the fibers of the nasofrontal suture in this plane were often difficult to visualize and varied both within and between individuals. As seen in Figure 6c, it was not possible to identify any primary fiber orientation in the nasofrontal suture or to characterize it as either compression or tension resistant.

Sutural growth

The margins of the interfrontal and internasal sutures exhibited two bands of fluorescing label, representing the bone mineralized during the two injections in the week prior to euthanasia (Fig. 7). In these sutures the tips of the interdigitating processes typically had thicker deposits of labeled bone than the intermediate straight sections, indicating that more growth occurred at the tips. Also, there were instances of slow growth and/or resorption in nearly all interfrontal and internasal sutures, as evidenced by areas with one label (calcein) or no label at all. In contrast, there was no evidence of localized areas of slow growth or resorption in the nasofrontal suture, which exhibited thick bands of labeled bone.

Quantitative comparison of growth rates using the total labeled areas (see Materials and Methods) showed clear differences among the sutures (Table 4). Growth rate was least in the posterior internasal suture (39.2 μm ± 11.4 SD), intermediate in the interfrontal (65.5 μm ± 14.0), and greatest in the nasofrontal (133.8 μm ± 50.9). The rate of growth of the nasofrontal suture was significantly greater than that of either the internasal or the interfrontal sutures (ANOVA/Tukey Test; $P = 0.001$ and $P = 0.01$, respectively), which in turn were not found to be different from each other. This finding is highly robust, considering that the direct linear method of growth assessment used in this suture was shown to underestimate growth as determined by the measurement of the total area of labeled bone used in the internasal and interfrontal sutures (see Materials and Methods). Although the ANOVA/Tukey did not show

a significant difference between the internasal and interfrontal sutures, both independent and paired *t*-tests did indicate that the interfrontal was growing faster ($P = 0.05$). This comparison is valid because these two sites were measured using the same methodology. Within the internasal suture, there appeared to be a trend for the middle location to grow more slowly than the other sites, but sample size was too small for statistical comparisons.

The extremely high growth rate was not the only distinguishing feature of the nasofrontal suture. The appearance of this bone was different from that of the other sutures. The new sutural bone of the undecalcified nasofrontal specimens was well mineralized, but had an almost porous appearance with many closely spaced lacunae. The decalcified sections showed numerous large and closely spaced cells in the areas of particularly rapid growth, e.g., the tips of interdigitations (Fig. 8). This texture and morphology was unique to the nasofrontal suture. The internasal and interfrontal sutures showed primary vascular bone, with sparsely distributed cells at growing bone surfaces.

DISCUSSION

The in vivo strains documented for the pig rostrum are among the largest recorded for mammalian sutures. Further, the results confirm the finding from the zygomatic suture (Herring and Mucci, ’91) that adjacent sutures can be under large strains of opposite polarity. Interestingly, the rostral sutures were predominantly compressed, in contrast to the tensile strains that characterize the braincase roof (Herring and Teng, submitted). The finding of tensile strains in the interfrontal suture (most anterior part of the braincase) is consistent with these previous results.

The forces that engender these sutural strains are those of mastication, muscle contraction, bite force, and possibly reaction loads at the jaw joints. The large masseter muscle is well situated to separate the frontal bones and indeed does so when electrically stimulated (Herring and Teng, submitted), thus suggesting that it is responsible for the tensile reading in the interfrontal suture during mastication in the present study. The consistent finding of compression at the internasal suture is more difficult to explain. This suture is close to the teeth but distant from the masticatory muscles, so internasal compression may be caused by medially directed forces transmitted via the maxilla from molar contact. If this is the case, then the idea that the rostrum is twisted opposite the cranium about an anteroposterior axis (Greaves, ’85) is supported. Twisting or shearing is also suggested by the alternating sign of internasal strain in pig number 254. However, these uniaxial data alone cannot provide a rigorous test of this hypothesis; such a test will be possible in a future study when the sutural strain data are combined with rosette strain data recorded from the maxilla and nasal bones during mastication and muscle stimulation.

Single-element gauges cannot accurately report strain magnitude except in the (unlikely) absence of shearing or torsional components. Nevertheless, we believe that the tension to compression ranking of interfrontal-internasal-nasofrontal is correct, recalling that shearing loads would add to the reported tension. Unlike the other locations, the interfrontal suture never showed compressive strain and so must have been the most tensed. Furthermore, the nasofrontal suture showed higher levels of compressive strain than did the internasal, so either it was indeed more compressed or it was less sheared. But it seems obvious that the nasofrontal suture was under high, not low, shear strain, given that the frontal bones are being separated and the nasal bones are being pushed together.

Our predictions regarding suture strain and morphology were generally borne out. Suture strains were correlated with interdigitation (data from Tables 2 and 3 yield $r = -0.91$, $P = 0.085$ for averages [n = 4] and $r = -0.77$, $P = 0.001$ for all locations [n = 16]). This association remains

even if the interfrontal sites are dropped and only the compressively strained locations are considered ($r = -0.77$, $P = 0.009$ [n = 10]). Thus, the greater the compressive strain, the more the interdigitation. In contrast, interdigitation does not seem to be important for the tensed interfrontal suture. Interdigitation was not correlated with growth rate ($r = -0.20$, $P = 0.75$ [n = 5] for averages and $r = -0.28$, $P = 0.26$ [n = 18] for all locations; Tables 3 and 4), indicating that this alternate explanation for morphology (Koskinen et al., '76) is incorrect.

Sutural fiber architecture also reflected in vivo strains. As predicted, the collagen fibers within the compressively loaded sutures were arranged to resist this type of stress (Fig. 1A). The pattern of suture fiber arrangement within the interfrontal suture was not exactly that predicted for resisting tension (Fig. 1B), but was nevertheless consistent with tension resistance. In particular, at the interdigitating corners of the suture there were well-developed attachments which would provide resistance to the tension generated during mastication. Of course, these fibers are also positioned to resist the constant and much lower magnitude tensile forces produced by expansion of the brain during growth. However, brain growth was probably completed in the 4–6-month-old pigs used in this study.

It is possible that some of the differences in the sutural ligament between the interfrontal and internasal sutures may stem from a developmental difference between cranial and facial sutures. According to Pritchard et al. ('56), each facial bone is enveloped in periosteum (comprised of cambial and capsular layers) and surrounded by a loose mesenchymal tissue, whereas the bones of the cranial vault are covered on the endo- and ectocranial surfaces with dura/periosteum, but this fibrous coating does not extend around the leading edges of these bones. As a consequence, each facial bone approaches the other with this layer intact at the suture margin, resulting in a total of five layers (in order: cambial, capsular, mesenchymal, capsular, cambial). In contrast, the cranial vault bones approach with their cambial layers within an already differentiated fibrous membrane, the ectomeninx, resulting in three layers. According to Pritchard et al. ('56), when the bones of the cranial vault are in close proximity, the centrally located ectomeninx splits, resulting in a total of five layers, similar to that seen in the facial skeleton. Although no differences in cranial and facial suture structure during later growth have been previously reported, it is noteworthy that we only observed a thick, centrally located bundle of fibers within the interfrontal suture. The internasal suture had a looser central region that was frequently flanked by two regions of fiber bundles, perhaps homologous to the capsular layers described by Pritchard et al. ('56).

In contrast to our predictions about morphology, our prediction that sutural growth rates would be lower in those sutures experiencing more compression was not supported. Although a comparison of the internasal and interfrontal sutures does show the expected relationship (slower growth in the compressed internasal suture than in the tensed interfrontal suture), the nasofrontal suture does not follow this pattern. Indeed, the highly compressed nasofrontal suture grew the fastest (49% faster than the interfrontal suture and 60% faster than the posterior internasal suture). Interestingly, it was the two sutures with the high apparent *absolute* strains (the interfrontal and nasofrontal) that had the higher rates of growth. The rapid growth of the nasofrontal suture is in apparent conflict with previous results based on extrinsic forces (Wagemans et al., '88; Kokich, '92), which indicate that compression should significantly retard bone apposition at sutures. A resolution to this contradiction is suggested by the unusual histology of the nasofrontal area.

The newly mineralized bone in the undecalcified sections of the nasofrontal suture had a texture reminiscent of ossified cartilage and was different from the more consolidated appearance of growing bone in the other sutures. Other reports in the literature describe a chondroid tissue in sutures that matches our observations on the newly mineralized bone of the nasofrontal suture. Pritchard et al. ('56), followed by Moss ('58), recognized a tissue within some sutures with

large irregular cells and scanty matrix that lacked the more orderly appearance of definitive secondary cartilage and is transformed directly into bone rather than being replaced by endochondral bone formation. Chondroid tissue is well mineralized, has numerous irregular and confluent cell lacunae, and contains both Type I and II collagen (Beresford, '81; Goret-Nicaise and Dhem, '82; Goret-Nicaise et al., '88). In humans, chondroid tissue is present in all cranial sutures during fetal life and persists at least until the ninth month of postnatal life (Goret-Nicaise et al., '88). It has been estimated by fluorescent labeling in the cat mandible to grow at a linear rate of 44–67 μm/day (compared to 5.3–8.9 μm/day for lamellar bone) (Goret-Nicaise et al., '88). Although it has not been well studied, there is evidence that the formation of chondroid tissue may be associated with extrinsic mechanical forces or movements. Chondroid tissue develops in the peripheral regions of cartilage of mechanically unstable fractures and sometimes in regions of localized micromovement in mechanically stable fractures (Ashhurst, '92). Chondroid tissue is observed in zones where intrinsic growth of a bone is countered by extrinsic forces and where the speed of calcified tissue formation is high (e.g., the mandibular symphysis and cranial sutures) (Goret-Nicaise et al., '88). Our histological observations of morphology and rapid growth and our recordings of high compressive strain in the nasofrontal suture are consistent with the idea that this suture contains chondroid tissue. In turn, the presence of this specialized tissue may explain the ability of the nasofrontal suture to grow rapidly despite compressive loading.

Acknowledgments

Contract grant sponsor: National Institute of Dental Research; Contract grant number: PHS grant DE08513.

We thank Scott Pedersen and Zi Jun Liu for help with experiments and discussion, Patricia Emry for help with the histology, and Jay Decker for assisting with the photography.

LITERATURE CITED

Anton SC, Jaslow CR, Swartz SM. Sutural complexity in artificially deformed human (*Homo sapiens*) crania. J Morphol 1992;214:321–332. [PubMed: 1474599]

Ashhurst, DE. Macromolecular synthesis and mechanical stability during fracture repair. In: Hall, BK., editor. Bone: fracture repair and regeneration. Vol. 5. Boca Raton, FL: CRC Press; 1992. p. 61-121.

Beresford, WA. Chondroid bone, secondary cartilage and metaplasia. Baltimore: Urban and Schwarzenberg; 1981.

Biewener AA, Taylor CR. Bone strain: a determinant of gait and speed? J Exp Biol 1986;123:383–400. [PubMed: 3746195]

Foley WJ, Kokich VG. The effects of mechanical immobilization on sutural development in the growing rabbit. J Neurosurg 1980;53:794–801. [PubMed: 7441340]

Goret-Nicaise M, Dhem A. Presence of chondroid tissue in the symphyseal region of the growing human mandible. Acta Anat 1982;113:189–195. [PubMed: 7124333]

Goret-Nicaise M, Manzanares PB, Nolmans E, Dhem A. Calcified tissues involved in ontogenesis of the human cranial vault. Anat Embryol 1988;178:399–406. [PubMed: 3177893]

Greaves WS. The mammalian postorbital bar as a torsion-resisting helical strut. J Zool Lond 1985;207:125–136.

Herring SW. Sutures — a tool in functional cranial analysis. Acta Anat 1972;83:222–247. [PubMed: 5085471]

Herring SW, Mucci RJ. In vivo strain in cranial sutures: the zygomatic arch. J Morphol 1991;207:225–239. [PubMed: 1856873]

Huang X, Zhang G, Herring SW. Alterations of muscle activities and jaw movements after blocking individual jaw-closing muscles in the miniature pig. Arch Oral Biol 1993;38:291–297. [PubMed: 8517800]

Jaslow CR. Sexual dimorphism of cranial suture complexity in wild sheep (*Ovis orientalis*). Zool J Linn Soc 1989;95:273–284.

Jaslow CR. Mechanical properties of cranial sutures. J Biomech 1990;23:313–321. [PubMed: 2335529]

Kokich, VG. Sutural response to orthopedic forces. In: McNamara, JA., editor. Bone biodynamics in orthodontic and orthopedic treatment. Vol. 27. Ann Arbor: Center for Human Growth and Development, University of Michigan; 1992. Craniofacial growth ser

Koskinen, L. Dissertation Thesis. University of Turku; Turku, Finland: 1977. Adaptive sutures: changes after unilateral masticatory muscle resection in rats. A microscopic study.

Koskinen L, Isotupa K, Koski K. A note on cranio-facial suture growth. Am J Phys Anthropol 1976;45:511–516. [PubMed: 998768]

Markens IS, Oudhof HAJ. Morphological changes in coronal suture after replantation. Acta Anat 1980;107:289–296. [PubMed: 7395447]

Moss ML. Experimental alteration of sutural area morphology. Anat Rec 1957;127:569–590. [PubMed: 13425015]

Moss ML. Fusion of the frontal suture in the rat. Am J Anat 1958;102:141–166. [PubMed: 13545186]

Moss ML. Extrinsic determination of sutural area morphology in the rat calvaria. Acta Anat 1961;44:263–272. [PubMed: 13773137]

Oudhof HAJ. Sutural growth. Acta Anat 1982;112:58–68. [PubMed: 7080799]

Persson M. The role of movements in the development of sutural and diarthrodial joints tested in long-term paralysis of chick embryos. J Anat 1983;137:591–599. [PubMed: 6654748]

Pritchard JJ, Scott JH, Girgis FG. The structure and development of cranial and facial sutures. J Anat 1956;90:73–86. [PubMed: 13295153]

Todd, TW.; Cooke, EV, Jr. The later developmental features of the skull of Sus barbatus barbatus. London: Proc Zool Soc; 1934. p. 685-696.

Wagemans PAHM, van de Velde JP, Kuijpers-Jagtman AM. Sutures and forces: a review. Am J Orthod Dentofacial Orthop 1988;94:129–141. [PubMed: 3041795]

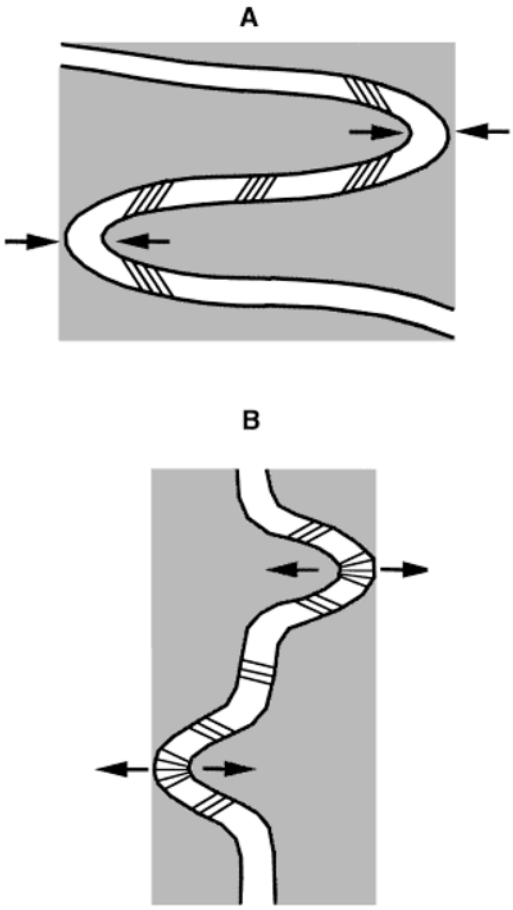

Fig. 1.
Schematic drawings of the expected bony and fibrous morphology of compressed and tensed sutures. **A:** A compressed suture with deep interdigitating processes and compression-resistant collagen fiber arrangement. **B:** A tensed suture with shallow interdigitating processes and tension-resistant collagen fiber arrangement.

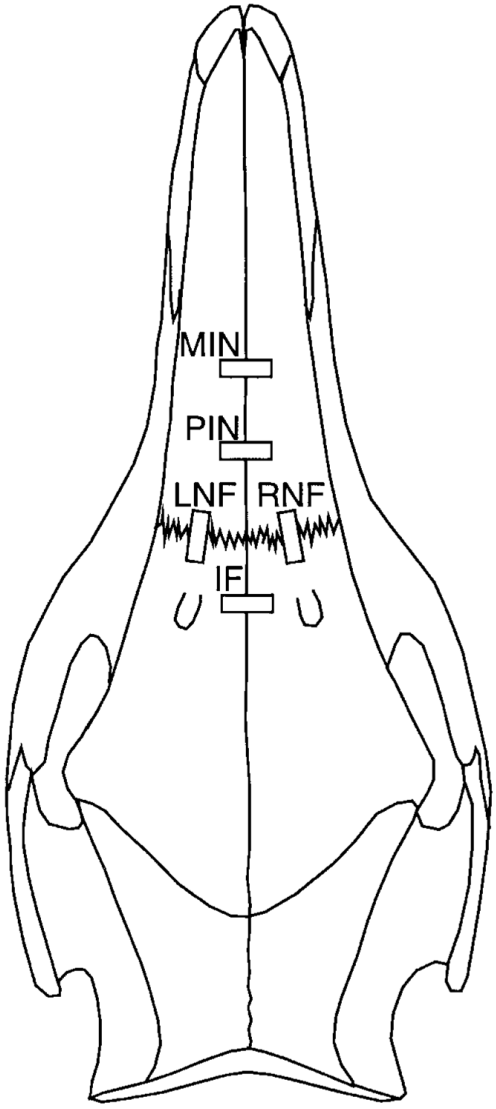

Fig. 2.
Sus scrofa. Dorsal view of skull showing the locations of the strain gauges across sutures of the braincase and rostrum. IF, interfrontal; MIN, mid-internasal; PIN, posterior-internasal; and RNF/LNF, right and left nasofrontal.

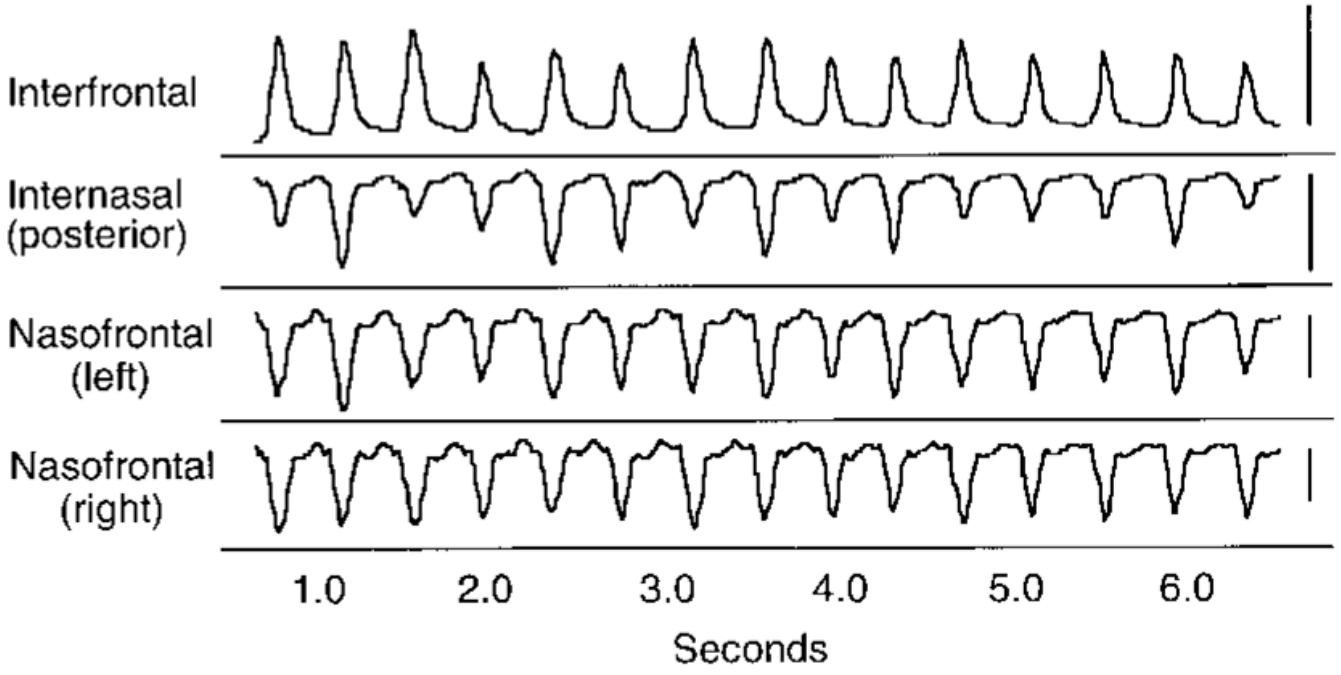

Fig. 3.

Sus scrofa. An example of typical strain recordings from sutures. Each peak corresponds to a masticatory cycle. The scale bar on the right is equivalent to one volt or 1,000 microstrain. Note that the interfrontal suture is in tension, whereas the other sutures are in compression. Data from pig 252.

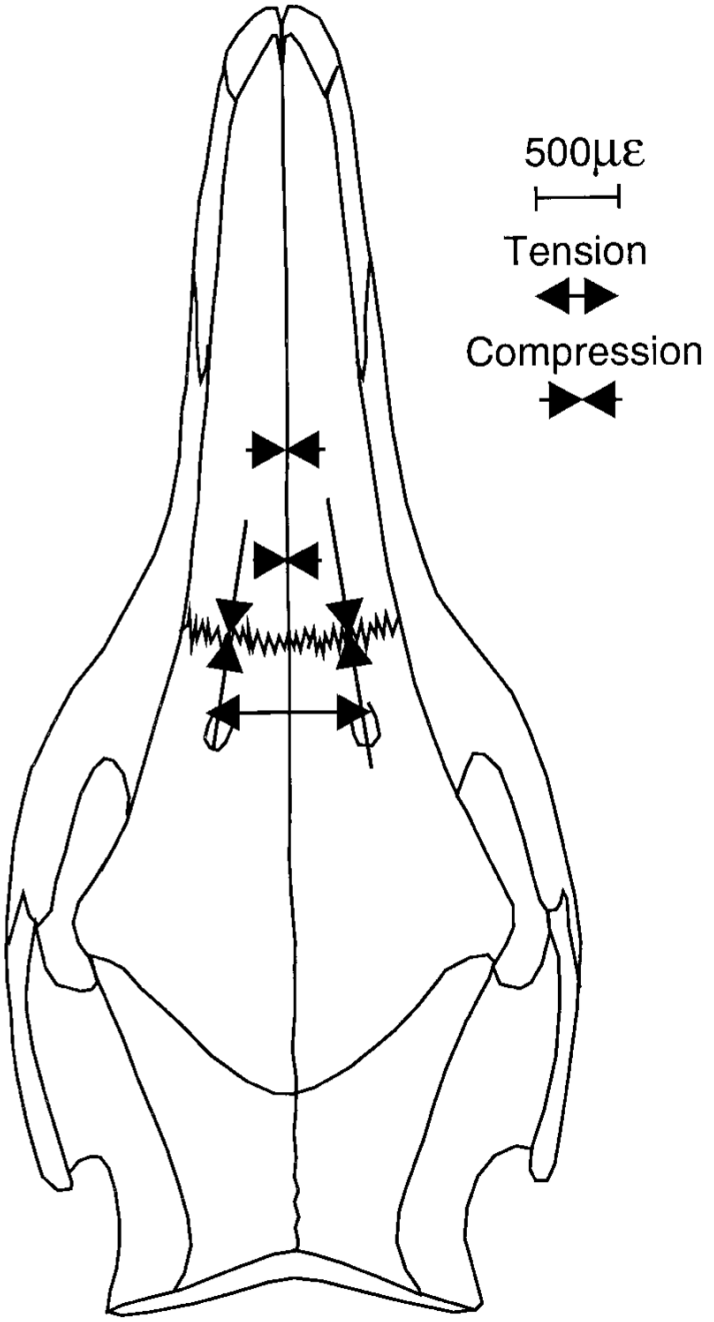

Fig. 4.
Sus scrofa. Dorsal view of skull with a schematic illustration of the average strains recorded from the interfrontal, internasal, and nasofrontal sutures.

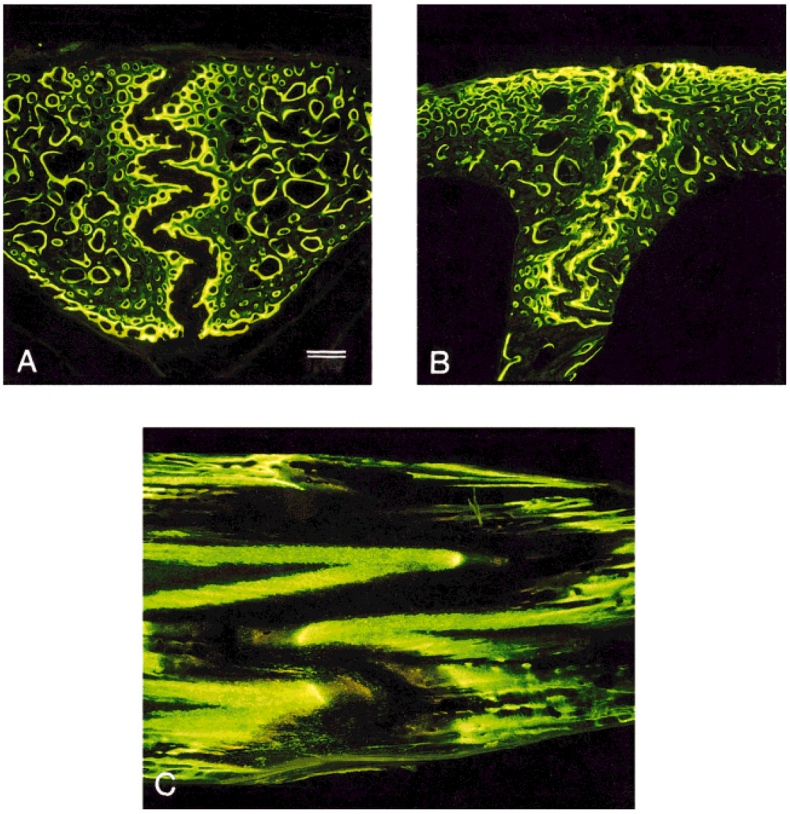

Fig. 5.

Sus scrofa. Double-labeled sutures under UV light at low magnification. **A:** Internasal suture in frontal section. **B:** Interfrontal suture in frontal section. **C:** Nasofrontal suture in sagittal section, frontal bone on left and nasal bone on right. Note the differences in interdigitation between these sutures and particularly the large size and distinct appearance of the nasofrontal suture. Scale bar = 500 μm.

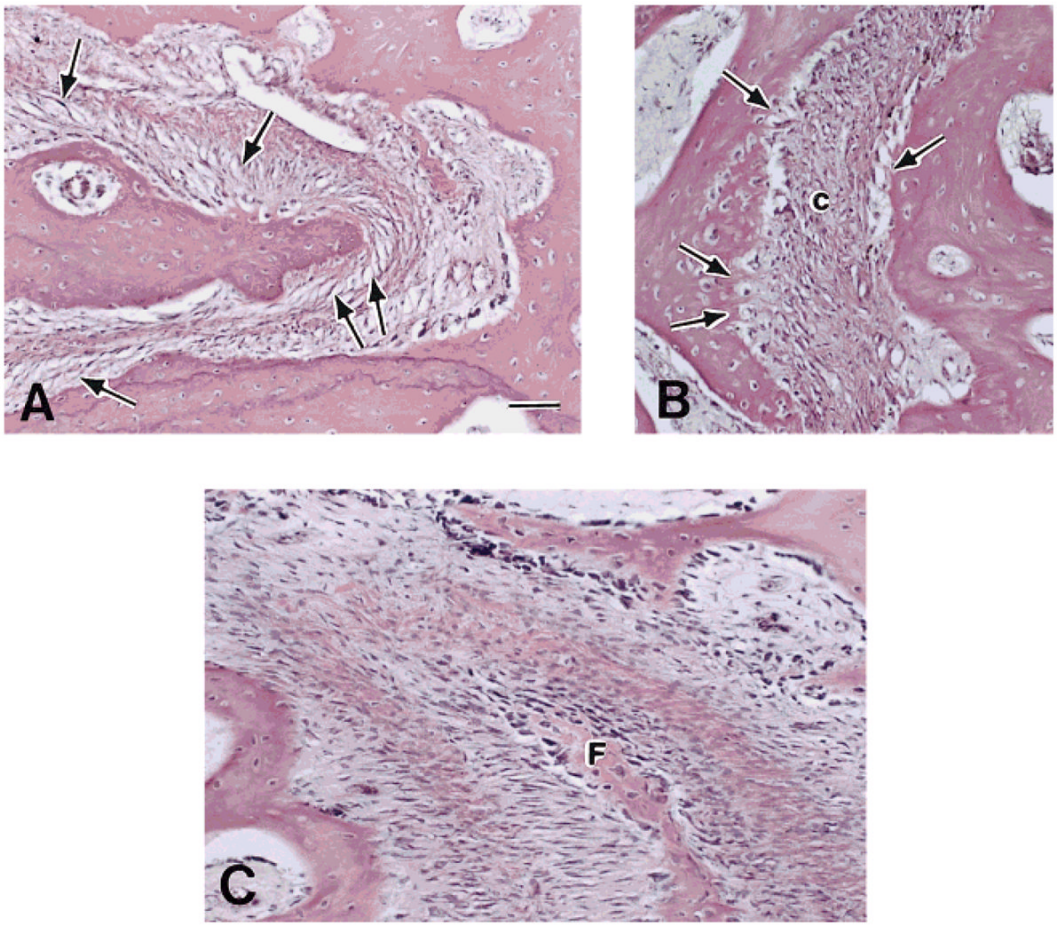

Fig. 6.

Sus scrofa. Sutures under transmitted light microscopy. **A:** Internasal suture. Note the obliquely arranged fibers within the suture space (arrows); their orientation is suited to resist compression. The central network is loosely organized. **B:** Interfrontal suture. Note the attachment of fibers (arrows) into the opposing sides of the suture space in a tension-resisting arrangement. The central network (c) is relatively compact and forms a dense bundle of fibers. **C:** Nasofrontal suture. Note complex and dense arrangement of collagen fiber bundles. The interdigitating tip belongs to the frontal bone (F). H&E stained thin sections. Scale bar = 50 μm.

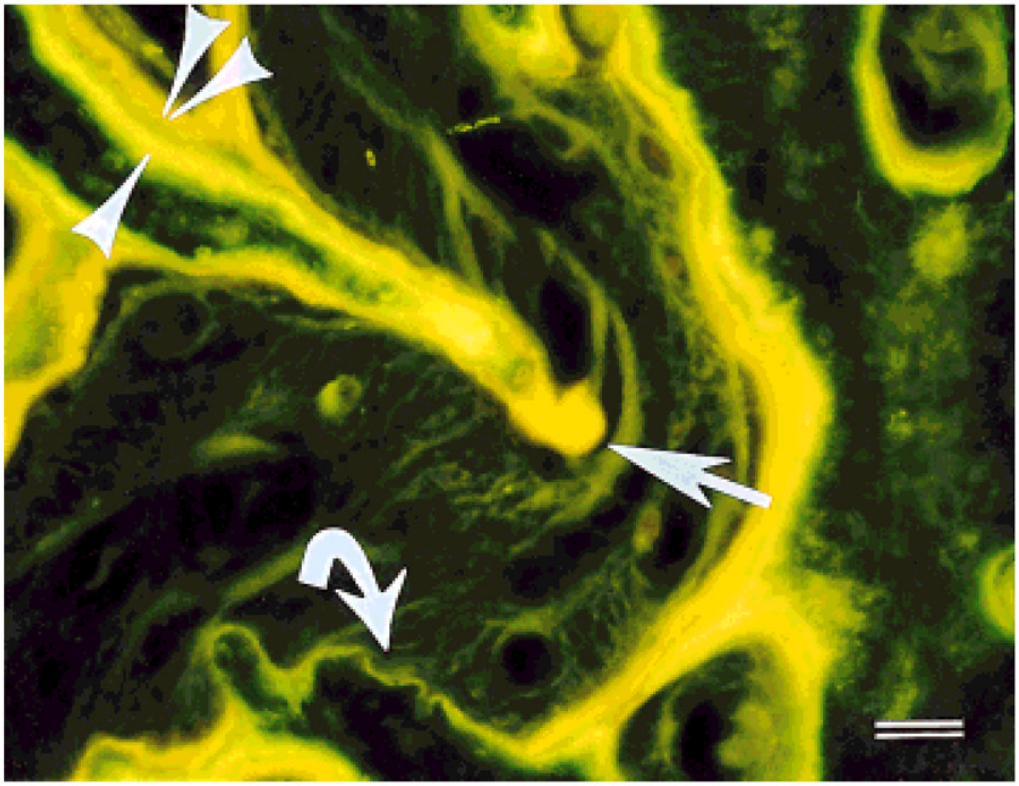

Fig. 7.

Sus scrofa. Double-labeled suture under UV light. The first label was calcein (yellow-green, single arrowhead) and the second label was demeclocycline (orange-yellow, double arrowhead). Note the variation in thickness of these labels from the greatest thickness in the interdigitating process (straight arrow) to the absence of the second label (curved arrow). Scale bar = 50 μm

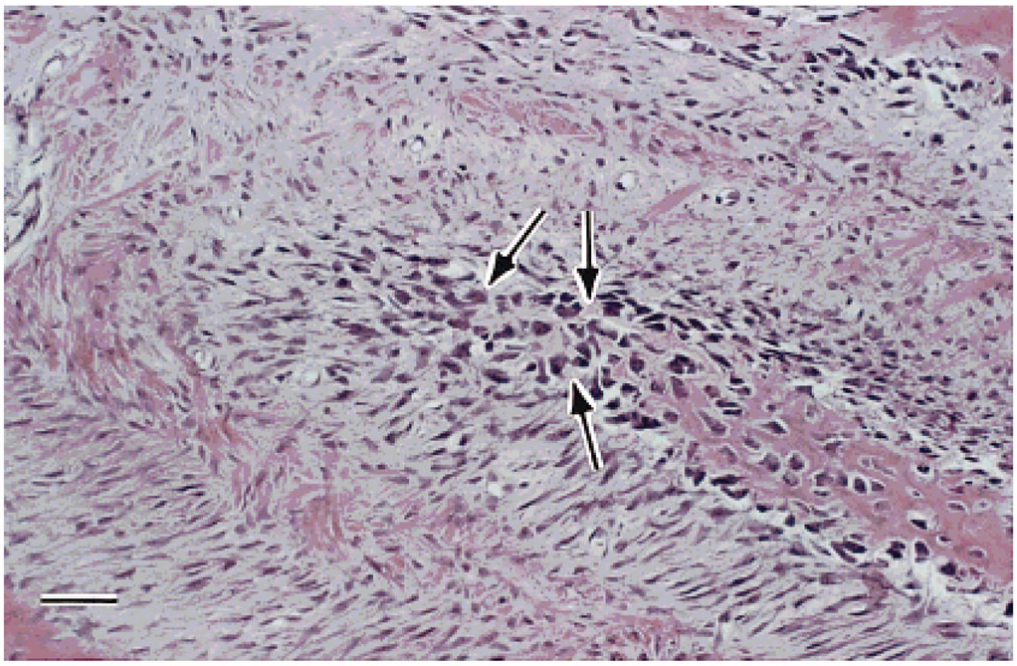

Fig. 8.

Sus scrofa. H&E stained thin section of the nasofrontal suture. Within the projection of bone (lower right to center) note the numerous large irregular darkly stained cells (arrows) believed to be indicative of chondroid bone. Scale bar = 50 μm.

TABLE 1

Subjects and strain gauge locations

			Internasal suture				Nasofrontal suture	
Pig no.	**Sex**	**Weight (Kg)**	**Anterior**	**Middle**	**Posterior**	**Interfrontal suture**	**Left**	**Right**
242	F	22.0	X*		X	X		
243	F	27.0	X*		X	X		
252	M	18.5			X	X	X	X
253	M	13.0			X	X	X	X
254	M	20.0		X	X	X	X	
255	F	23.0		X	X	X	X	

*Masticatory strains not available but growth and morphology data taken from this location.

TABLE 2

Peak suture strains (mean με and SD) during mastication

		Internasal suture			Nasofrontal suture	
Pig no.	**No. of chews**	**Middle**	**Posterior**	**Interfrontal suture**	**Left**	**Right**
242	14		−446 (82)	776 (168)		
243	11		−230 (43)	611 (36)		
252	14		−761 (224)	706 (119)	−1,413 (158)	−2,017 (162)
253	14		−503 (38)	1,283 (121)	−480 (76)	−1,254 (321)
254	16	−266 (239)	−109 (176)*	1,215 (138)	−1,912 (1023)	
255	24	−706 (315)	−590 (331)	1,628 (273)	−1,869 (888)	
Mean		−486	−440	1,036	−1,583	
SD		311	238	400	506	

*The posterior internasal suture of this animal registered small tensile strains (<100 με) when chewing on one side and moderate compressive strains when chewing on the other side.

TABLE 3

Suture interdigitation index[1]

	Internasal suture				
Pig no.	**Anterior**	**Middle**	**Posterior**	**Interfrontal suture**	**Nasofrontal suture[2]**
242	2.0	3.4	2.2	1.6	
243	1.8		2.3	1.5	3.3
252			2.0	2.4	5.8
253			2.7	1.7	3.2
254		2.6		1.8	
255		3.4	2.0	1.5	3.7
Mean	1.90	3.13	2.24	1.75	4.00[3]
SD	0.14	0.46	0.29	0.34	1.22

[1] Suture interdigitation index = true suture length/shortest distance between endo- and ectocranial surfaces.

[2] Data are from right or left side.

[3] ANOVA/Tukey test: nasofrontal vs. posterior internasal $P = 0.005$; nasofrontal vs. interfrontal $P = 0.001$.

TABLE 4

Weekly suture growth (μm)

	Internasal suture				
Pig no.	**Anterior**	**Middle**	**Posterior**	**Interfrontal suture**	**Nasofrontal suture**
242	44.0	39.0	52.0	64.0	
243	53.0		44.0	83.0	206.0
252			39.0	50.0	74.0
253			40.0	52.0	134.0
254		24.0		81.0	100.0
255		26.0	21.0	63.0	155.0
Mean	48.5	29.7	39.2	65.5	133.8*
SD	6.4	8.1	11.4	14.0	50.9

*ANOVA/Tukey test: nasofrontal vs. posterior internasal $P = 0.001$; nasofrontal vs. interfrontal $P = 0.01$.